Pergamon

Chemical Engineering Science, Vol. 53, No. 18, pp. 3215–3225, 1998

Printed in Great Britain
0009-2509/98/$-See front matter

PII: S0009-2509(98)00105-5

Die entry pressure drops in paste extrusion

D. J. Horrobin and R. M. Nedderman*

Department of Chemical Engineering, University of Cambridge, Pembroke Street, Cambridge CB2 3RA, U.K.

Received 24 July 1997; in revised form 1 April 1998

Abstract—Pressure drops for the extrusion of a perfectly plastic material through smooth-walled dies with various reduction ratios and conical entry angles have been calculated by the large deformation elastic–plastic finite element method. They are found to agree well with extrusion pressures obtained from slipline field analyses for plane strain problems, and lie within the limits set by upper- and lower-bound solutions in axisymmetric cases. The results for axisymmetric dies are compared with the die entry pressure drop term in the Benbow–Bridgwater equation, used to describe the flow of pastes in a ram extruder. © 1998 Elsevier Science Ltd. All rights reserved.

INTRODUCTION

Benbow and Bridgwater (1993) describe a simple model for the flow of pastes in a ram extruder (Fig. 1). If the material is thought to behave as a perfect plastic in the bulk, and the work done in the die entry region is identical to that for homogeneous compression between parallel plates, the die entry pressure drop is given by

$$P_1 = 2\sigma_y \ln\left(\frac{D_0}{D}\right) \tag{1}$$

where σ_y is the uniaxial yield stress, D_0 is the barrel diameter, and D is the die land diameter; it is assumed that the barrel and die land both have circular cross-sections. This expression is applied to dies with abrupt contractions (square entry dies), and to dies with conical or tapered entries when wall friction is not thought to be significant. Ovenston and Benbow (1968), and Benbow (1971) present experimental results for the extrusion of ceramic pastes through square and conical entry dies, and argue that the effect of geometry on the die entry pressure drop is consistent with eq. (1).

In homogeneous compression, a rectangular element in the undeformed specimen, with sides parallel to the principal directions of stress and strain, remains rectangular in the deformed state. In this case, all the energy supplied via the platens results in a change in the height of the specimen, and the work done is a minimum, termed ideal work. During extrusion, the deformation in the die entry region is not homogeneous, with additional work going into shearing material elements without causing a reduction in the overall diameter. The additional work is termed redundant work, and causes the die entry pressure drop to be in principle rather greater than that predicted by eq. (1).

It is often found experimentally that P_1 exhibits some rate dependence, and eq. (1) is modified by Benbow and Bridgwater (1993) as follows:

$$P_1 = 2(\sigma_0 + \alpha V)\ln\left(\frac{D_0}{D}\right) \tag{2}$$

where V is the velocity of the paste in the die land, σ_0 is an initial yield stress, and α is a parameter characterising the effect of velocity in the die entry. Both σ_0 and α are regarded as material constants, and are assumed to be independent of die geometry and extrusion rate.

In the die land the paste flows as a rigid plug, possibly surrounded by a thin layer of lubricating liquid separating it from the wall. Thus, the wall shear stress may be a function of the velocity of the plug, and the die land pressure drop is given by

$$P_2 = 4(\tau_0 + \beta V)\frac{L}{D} \tag{3}$$

where L is the die land length, τ_0 is an initial wall stress, and β is a parameter characterising the effect of velocity in the die land; τ_0 and β are also regarded as material constants. Adding the pressure drops (2) and (3) together leads to the four-parameter model for the overall pressure drop, sometimes known as the Benbow–Bridgwater equation.

$$P = 2(\sigma_0 + \alpha V)\ln\left(\frac{D_0}{D}\right) + 4(\tau_0 + \beta V)\frac{L}{D}. \tag{4}$$

The relative roughness of the wall in the die land may be assessed by comparing τ_0 with the shear yield

*Corresponding author. Tel.: 01223 334777; fax: 01223 334796.

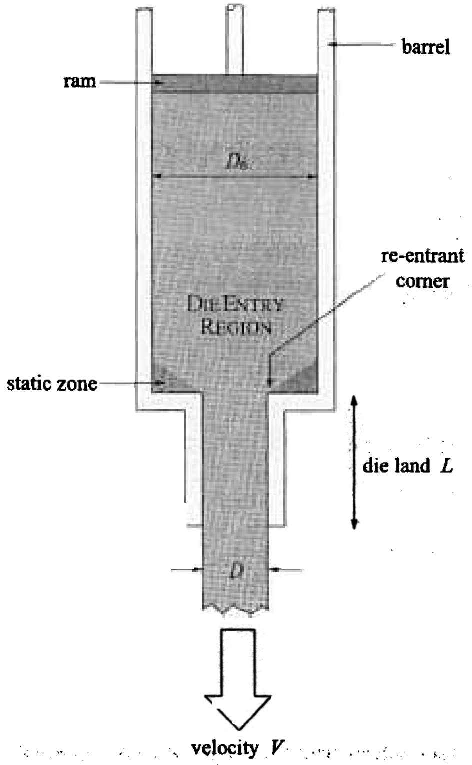

Fig. 1. A simple ram extruder with a square entry die.

stress of the material, as this is the maximum shear stress that can be sustained by a perfect plastic. The shear yield stress τ_y is expected to be about half the uniaxial yield stress: Tresca's yield criterion predicts that τ_y is equal to $\sigma_y/2$, while von Mises' criterion predicts that τ_y is equal to $\sigma_y/\sqrt{3}$. In practice, the magnitudes of σ_0 and τ_0 depend on the composition of the paste, but for ceramic pastes it is often found that τ_0 is an order of magnitude less than σ_0. The interaction between the paste and the wall in the die land is therefore of a rather smooth nature, at least for low extrusion rates, presumably as a result of the lubricating layer of liquid. However, the same boundary condition does not automatically apply to the flow in the die entry.

Several authors have made use of the finite element method to study the extrusion of plastic materials in the context of metal-forming processes. Two formulations are commonly encountered: the flow approach, and the elastic–plastic or solid approach. In the flow formulation, elastic strains are completely neglected on the grounds that the plastic strains are very much greater in problems that involve large deformations. The material is considered to be a viscous, non-Newtonian fluid, and the primary variables in the calculation are velocities at the nodes of the finite element mesh. For a material obeying von Mises' yield criterion and associated flow rule, the viscosity given by Zienkiewicz *et al.* (1978) is

$$\mu = \frac{\sigma_y}{\sqrt{3}\dot{\bar{\varepsilon}}} \tag{5}$$

where $\dot{\bar{\varepsilon}}$ is the effective strain rate. In regions where the material is undergoing rigid-body motion, $\dot{\bar{\varepsilon}}$ tends to zero and the viscosity tends to infinity. In practice, a large but finite cut-off value for the viscosity is applied, and the material is thus treated as a highly viscous Newtonian fluid wherever the stress is below the yield point.

Zienkiewicz *et al.* (1978) presented results for plane strain extrusion of a non-hardening von Mises material through smooth- and rough-walled square entry dies. In the smooth-walled case, the calculated extrusion pressures gave good agreement with those obtained from slipline field solutions. They also examined axisymmetric pipe extrusion, in both forward and inverted configurations, and found good agreement between calculated extrusion pressures and experimental values. Chen *et al.* (1979) investigated the extrusion of both hardening and non-hardening materials through axisymmetric conical entry dies, with the principal aim of comparing different criteria for ductile fracture. A plot of P/σ_y against $\ln(D_0/D)$ for smooth-walled dies with a 45° entry angle was found to produce a straight line. However, in contrast with the behaviour predicted by eq. (1), this line had a positive intercept when extrapolated to a $\ln(D_0/D)$ value of zero, and for the non-hardening material the value of the slope was less than two.

In the elastic–plastic formulation, elastic strains are not neglected, and the primary variables are nodal displacements rather than velocities. A Lagrangian mesh, deforming with the material, is used in an incremental analysis. The equilibrium relationships are expressed in terms of a reference geometry, and the elastic–plastic schemes may be further divided into two categories depending on the reference geometry chosen. In the total Lagrangian formulation, the reference geometry is taken as the initial configuration of the material, while in the updated Lagrangian formulation, the reference geometry is the configuration at the beginning of the current time increment. The solid approach is rather more complicated than the flow approach, as extra care is needed to properly account for the effect of geometrical non-linearities (large displacements and strains) as well as material non-linearities. A particular difficulty surrounds the choice of an appropriate objective stress rate for use in the elastic–plastic constitutive relationships (Voyiadjis and Foroozesh, 1991). The principal advantage of this approach is seen as the ability to predict the stress field in regions where the material is not at the yield point, particularly the residual stresses in parts that have experienced unloading.

An early example of the application of the large strain elastic–plastic method to extrusion problems is the work of Lee *et al.* (1977). Here, an updated Lagrangian scheme was used to study the plane strain extrusion of an aluminium billet through a smooth-walled curvilinear die. The billet, modelled as a strain-hardening von Mises material, experienced a 25% reduction in width in a distance of 0.6 times the initial width; this corresponds to an approximate

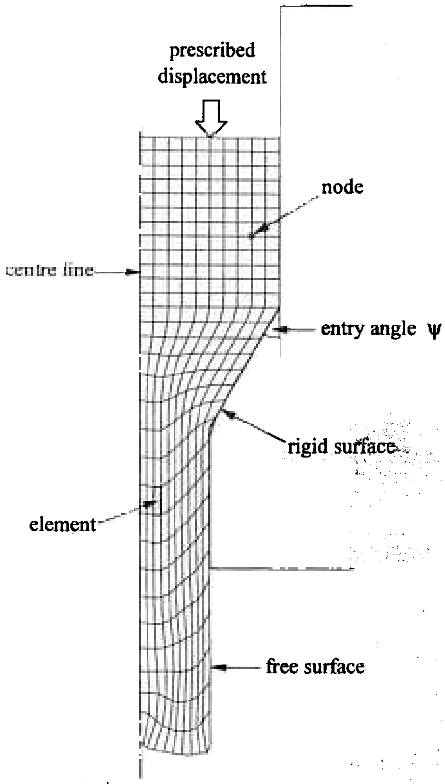

Fig. 2. Finite-element mesh for plane strain extrusion through a smooth, tapered entry die with a 30° entry angle and a 50% reduction in width.

angle of taper ψ (defined in Fig. 2) of 11.8°. In addition to calculating the extrusion pressure, the stress field in the deforming zone and the residual stresses in the extrudate were also discussed. Nagtegaal and Veldpaus (1984) considered the axisymmetric analogue of this problem, again using an updated Lagrangian scheme. They calculated the extrusion pressure for a slightly work-hardening material extruded through a smooth curvilinear die with a 25% area reduction. Voyiadjis and Foroozesh (1991) employed a total Lagrangian formulation to study the axisymmetric extrusion of a work-hardening aluminium alloy, their justification for adopting the total Lagrangian scheme being that it circumvented the difficulty of choosing an objective stress rate. They also considered smooth curvilinear dies, and investigated a range of area reductions between 25 and 35%, and approximate angles of taper between 5 and 9°. They concluded that the extrusion pressure increased linearly with angle, and approximately linearly with area reduction.

For paste flows the constitutive behaviour of the material below the yield point is not well established. Unlike the situation in metal forming, it is not clear that Hooke's Law provides an appropriate description, and the flow formulation, in which the material is treated as a Newtonian fluid below the yield point, may be more realistic than the elastic–plastic approach. However, the extrusion pressure seems to be determined by processes occurring in the deformation zone, where the material is at the yield point, and both formulations are expected to give the same results where this aspect of the problem is concerned.

As far as the present authors are aware, there has been no numerical study of how extrusion pressure depends on die geometry for axisymmetric dies for the range of reductions and entry angles encountered in paste extrusion. This paper describes how the elastic–plastic finite-element method has been used to calculate these loads, and compares the results with the first term in the Benbow–Bridgwater equation.

CALCULATION PROCEDURE

The basis for the calculations described in this paper is the ABAQUS Finite Element Package, Version 5.5 (Hibbitt, Karlsson and Sorensen, Inc., 1995). An incremental analysis is performed, in which a Lagrangian mesh (Fig. 2), comprised of four-noded quadrilateral elements, is used to represent an elastic, perfectly plastic billet as it travels through the die under the influence of a ram. The elastic response of the material is modelled using Hooke's law, and von Mises' yield criterion and associated flow rule are employed to describe the plastic deformation. The extrusion pressure can be obtained at any time during the analysis by integrating the longitudinal stress component over the area of the ram. For an axisymmetric problem, the pressure is given by

$$P = \frac{1}{\pi R_0^2} \int_0^{R_0} 2\pi r[-\sigma_l(r)]\,dr \qquad (6)$$

where R_0 is the radius of the barrel. This quantity may be calculated after each analysis increment and plotted against ram displacement to produce a pressure–displacement curve. Alternatively, the pressure may be obtained from the total energy dissipated during the increment by means of an energy balance.

In order to test the calculation procedure, several plane strain extrusion problems have been studied. In addition to the upper- and lower-bound estimates for the extrusion pressure available in the axisymmetric case, in plane strain the numerical results may be compared with accurate predictions from slipline field analyses. Two difficulties were found to arise during the calculations. Firstly, for extrusion through dies with a tapered entry, large oscillations were observed in the pressure–displacement curves where the extrusion pressure was expected to have a steady value. Secondly, for extrusion through square entry dies, gross distortion of the mesh occurs around the re-entrant corner, and the extrusion pressure displays very large, non-periodic variations.

Figure 3 shows the pressure–displacement curve for plane strain extrusion through a tapered entry die with a 30° entry angle and 50% reduction in width; the die and mesh for this problem are shown in Fig. 2. The large oscillations in the extrusion pressure can be identified with the passage of individual nodes around the corners of the die. Similar oscillations have been observed by Lee *et al.* (1977), Nagtegaal and Veldpaus

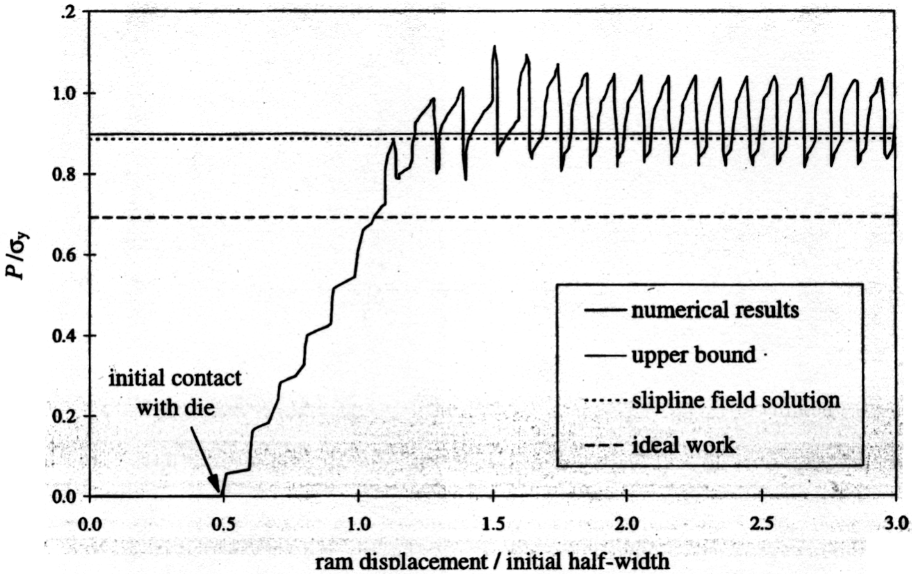

Fig. 3. Extrusion pressure against ram displacement for the die and mesh in Fig. 2.

(1984) and Voyiadjis and Foroozesh (1991). The pressure calculated from the slipline field solution (Chakrabarty, 1987a), is less than the mean value of the numerical pressures in the steady-state part of the curve, indicating that an accurate estimate of the extrusion pressure cannot be obtained by averaging over several oscillations. Also shown in Fig. 3 are the pressures obtained from upper- and lower-bound solutions for this geometry. The upper-bound solution, in which deformation is assumed to occur by a rigid-block mechanism with sliding along the die face, is described by Calladine (1985a). The lower-bound value is that obtained from the homogeneous work assumption: as in the axisymmetric case, the pressure is found by multiplying the uniaxial yield stress by the natural logarithm of the area ratio. Thus, for an initial width W_0 and a final width W,

$$P = \sigma_y \ln\left(\frac{W_0}{W}\right). \tag{7}$$

It can be seen in Fig. 3 that the amplitude of the oscillations is comparable to the difference between the upper- and lower-bound pressures, and so no improvement in accuracy is achieved by the relatively complicated numerical analysis compared with the simple predictions of the upper- and lower-bound solutions.

Figure 4 shows the distortion undergone by a regular square mesh in the early stages of extrusion through a square entry die. Here, the mesh provides an unphysical representation of the billet, in which some elements severely cut the re-entrant corner, and the corresponding pressure–displacement curve exhibits irregular variations and fails to reach a steady-state, with or without oscillations.

The problem of excessive distortion can be solved by remeshing the billet at relatively frequent intervals, replacing the misshapen elements with undistorted elements within the same material boundary. The solution from the previous analysis step is then mapped onto the new mesh, allowing the analysis to be continued. The problem of oscillations in the pressure–displacement curve can be alleviated simultaneously by making the elements small in regions where the rate of deformation is large (near the re-entrant corner in the case of square entry dies), but relatively large where the material is rigid. Thus, the total number of nodes in the mesh is kept to a minimum, and the calculation time is as short as possible.

A mesh generation program has been written by the authors that creates a new mesh, based on the solution from the previous analysis step, which is then supplied as part of the input for the next step. The remeshing is accomplished in several stages. Firstly, the desired distribution of element sizes is calculated, a size being associated with each node in the old mesh. This is then used as a background mesh on which the new elements are constructed. Several methods for choosing the element size distribution have been investigated. One of these is based on the method of Zienkiewicz and Zhu (1987) designed to create an optimal mesh that minimises the interpolation error in the energy dissipation field. An alternative, simpler scheme is to choose element sizes that are inversely related to the local rate of strain in the material. In all cases, a pre-determined element size is stipulated for elements near corners of the die (unless the rate of strain there is close to zero) to ensure that the mesh is sufficiently fine in these regions. Before the mesh is constructed a smoothing algorithm is applied to the size distribution to ensure that the sizes associated with adjacent nodes in the old mesh never differ by a factor of more than about two. All methods used for choosing the element size distribution are found to

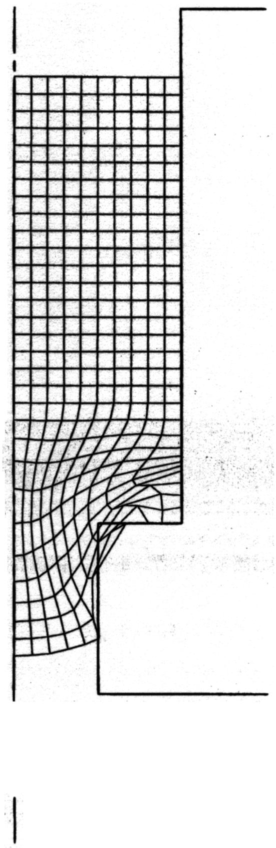

Fig. 4. Finite-element mesh for plane strain extrusion through a smooth, square entry die with a 50% reduction in width, showing distortion of initial grid.

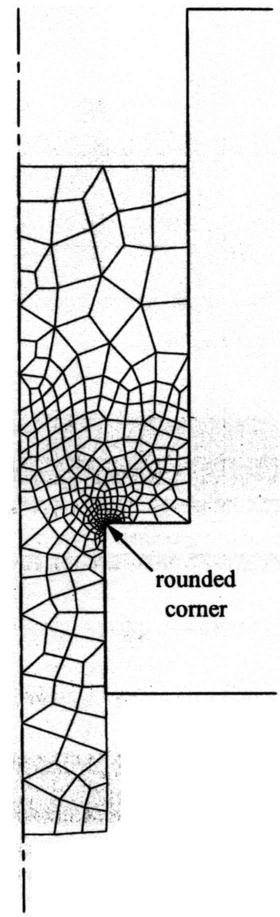

Fig. 5. Finite-element mesh for plane strain extrusion through a smooth, square entry die with a 50% reduction in width, showing variation in element size.

give rise to similar meshes, and ultimately to similar extrusion pressures.

A triangular mesh is generated, based on the advancing front technique described by Peraire *et al.* (1986). Most of the boundary nodes are retained between the old mesh and the new mesh. An exception occurs when the separation of adjacent boundary nodes has become rather smaller than the local desired element size, in which case a node will be deleted. Conversely, if the spacing of adjacent boundary nodes is much larger than the desired element size, an additional node will be created. Finally, a quadrilateral mesh is produced by merging pairs of adjacent triangles, followed by several mesh modification and smoothing steps; the procedure is based on that described by Lee and Lo (1994). At the beginning of the new step, the mapping of the old solution onto the newly created mesh is performed by the ABAQUS package.

To illustrate the improvement in the solution as a result of remeshing, plane strain extrusion through a smooth, square entry die with a 50% reduction in width is considered; a typical mesh for this problem is shown in Fig. 5. In this case, the slipline field solution is particularly simple, and the extrusion pressure is given by Chakrabarty (1987b):

$$P = \frac{\sigma_y}{\sqrt{3}}\left(1 + \frac{\pi}{2}\right). \tag{8}$$

To obtain reliable convergence of the solution algorithm, it is necessary to make the re-entrant corner slightly rounded. This rounding can be seen in Fig. 5, where the fillet radius at the corner is 1.5% of the barrel diameter. Rounding the corner alters the profile of the die, and hence the extrusion pressure, but tests with various fillet radii indicate that the difference is not significant for the level of rounding typically employed. As seen in Fig. 6, the pressure–displacement curve quickly reaches a steady state as the material starts to enter the die land, and exhibits small fluctuations about the mean value thereafter. The extrusion pressure is found by taking the average value of the points on this curve once the steady state has been reached, and the finite-element and slipline field extrusion pressures show excellent agreement. An upper-bound solution, based on a rigid-block mode of deformation with a static zone on the die face, is given by Calladine (1985b). It is noted that the difference between the upper bound and the slipline

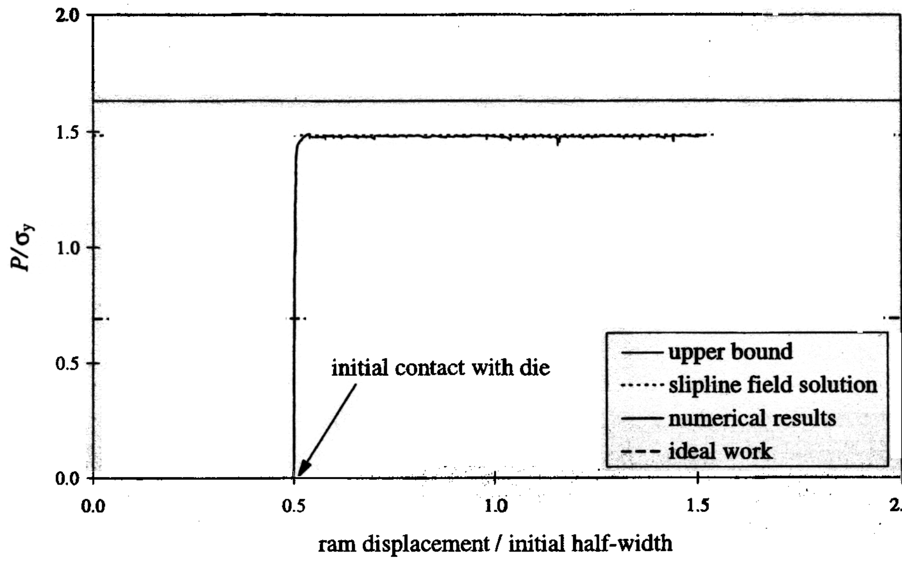

Fig. 6. Extrusion pressure against ram displacement for the die and mesh in Fig. 5.

field extrusion pressure is rather greater than that in Fig. 3 for a tapered entry die. Thus, for the square entry die, the bound theorem approach does not give such a clear indication of the extrusion pressure.

RESULTS

The material and mesh parameters selected for the analyses described in this section were as follows: The ratio of the material's Young's modulus to its uniaxial yield stress was between 10^2 and 10^5 in all cases. A large value for this ratio is appropriate for three reasons. Firstly, there is some evidence to suggest that the ratio is of order 10^3 for both ceramic pastes (Feasey and Wilson, 1996) and soaps (Garvey and Ross, 1996). Secondly, it validates an approximation used in ABAQUS, and more widely in the analysis of elastic–plastic deformations, that the total strain rate is the sum of an elastic contribution and a plastic contribution (the 'additive strain rate decomposition' — see the ABAQUS Theory Manual and e.g. Lee, 1984). Thirdly, we have observed that for the larger diameter reductions, the material in the barrel can undergo significant elastic volume change during an analysis increment, and that this effect is reduced by making the Young's modulus very much larger than the uniaxial yield stress.

The material's Poisson's ratio was chosen to be 0.49, this value being somewhat arbitrary, although a Poisson's ratio close to 0.5 results in the elastic part of the deformation being approximately volume-conserving. It is believed that changing the Poisson's ratio has very little effect on the extrusion pressures.

Typical meshes contained 300–800 nodes, with the smallest element size being of order 0.1% of the barrel diameter. The extrudate displacement during each analysis step (i.e. before remeshing) was between 0.1 and 2% of the barrel diameter, and the fillet radius at the re-entrant corner was less than 1.2% of the barrel diameter in all cases.

Table 1. Extrusion pressures for axisymmetric extrusion through smooth, square entry dies

Die land diameter	Diameter reduction (%)	P/σ_y
24	4	0.33
22	12	0.78
20	20	1.14
18	28	1.47
16	36	1.81
14	44	2.15
12	52	2.49
10	60	2.85
8	68	3.26
6	76	3.81
4	84	4.57
2	92	5.93

Note: Barrel diameter = 25 in all cases.

Square entry dies

Extrusion pressures have been calculated for axisymmetric flow through smooth, square entry dies, with diameter reductions of between 4 and 92%. The dimensionless pressures P/σ_y are given in Table 1, and are plotted against $\ln(D_0/D)$ in Fig. 7. As expected, the numerical values all lie above the straight line obtained by plotting P/σ_y from eq. (1), based on the ideal work assumption. An alternative lower-bound solution for smooth, square entry dies, proposed by Kobayashi and Thomsen (1965), is found to produce a better (i.e. higher) estimate for the extrusion pressure for diameter reductions less than about 75%, and this is also shown in Fig. 7. The upper-bound curve

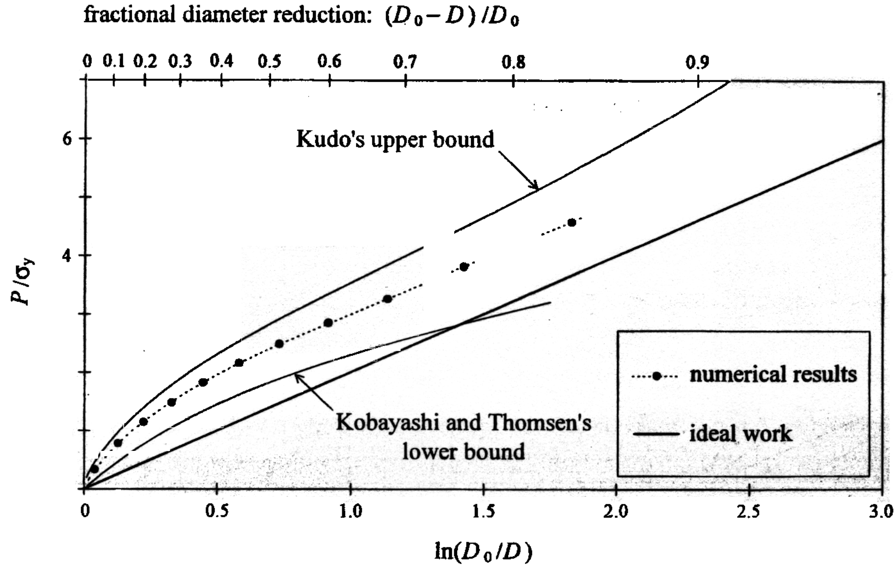

Fig. 7. Extrusion pressure against $\ln(D_0/D)$ for axisymmetric extrusion through smooth, square entry dies.

corresponds to a solution given by Kudo (1960). Kudo describes four different velocity fields appropriate for axisymmetric extrusion through square entry dies, and we have found that, of these, one produces either the best (i.e. lowest), or close to the best, estimate for the extrusion pressure at all reductions. This deformation mode has Kudo's 'parallel velocity field' in the outer part of the deforming region, and 'triangular velocity field' in the inner part.

For diameter reductions less than about 50%, the contribution made by redundant work to the overall extrusion pressure is comparatively large, and a reasonably good estimate of the pressure is provided by the upper-bound solution. However, as the reduction increases, the ideal work increases, while the redundant work remains roughly constant, and thus the ideal work assumption provides a better estimate for the extrusion pressure at large reductions.

A curve may be fitted through the calculated points in two sections as follows: the points lie roughly on a straight line for diameter reductions above 60%, and on a parabolic curve for smaller reductions. Writing ξ for $\ln(D_0/D)$, the best-fit parabola and straight line are found to be

$$P/\sigma_y = 0.700(\sqrt{26.8\xi + 1} - 1)$$

$$\text{diameter reduction} < 60\% \qquad (9)$$

$$P/\sigma_y = 1.92\xi + 1.08$$

$$\text{diameter reduction} \geqslant 60\%. \qquad (10)$$

These equations are also plotted in Fig. 7. The straight line for large reductions has a slope that is slightly less than two, and thus approaches the ideal work line as the reduction increases. A similar situation occurs in the analogous plane strain case, where the extrusion pressures may be obtained from slipline field analyses (Chakrabarty, 1987c). Since the ideal work line cannot be crossed, eq. (10) does not apply for arbitrarily large reductions. However, the intersection of the lines given by eqs (1) and (10) occurs at $\xi = 13.5$, corresponding to a diameter ratio D/D_0 of around 10^{-6}.

Table 2. Extrusion pressures for axisymmetric extrusion through smooth, conical entry dies with a 52% diameter reduction

Die entry angle (deg)	P/σ_y
5	1.49
15	1.55
30	1.65
45	1.84
60	2.06
75	2.28
90	2.49

Conical entry dies

Extrusion pressures have been calculated for smooth dies having diameter reductions of 52%, but with differing entry angles. In this case, large rates of strain may be apparent at both ends of the tapered die face, and small elements and rounding off are required at each corner. The angles investigated and pressures obtained are listed in Table 2, and a plot of extrusion pressure against entry angle is shown in Fig. 8.

Since the diameter reduction is the same for all the dies, the extrusion pressure calculated from the ideal work assumption has a constant value, and this provides a lower bound. The upper-bound curve has been obtained from a solution for conical entry dies described by Kobayashi and Thomsen (1965). We

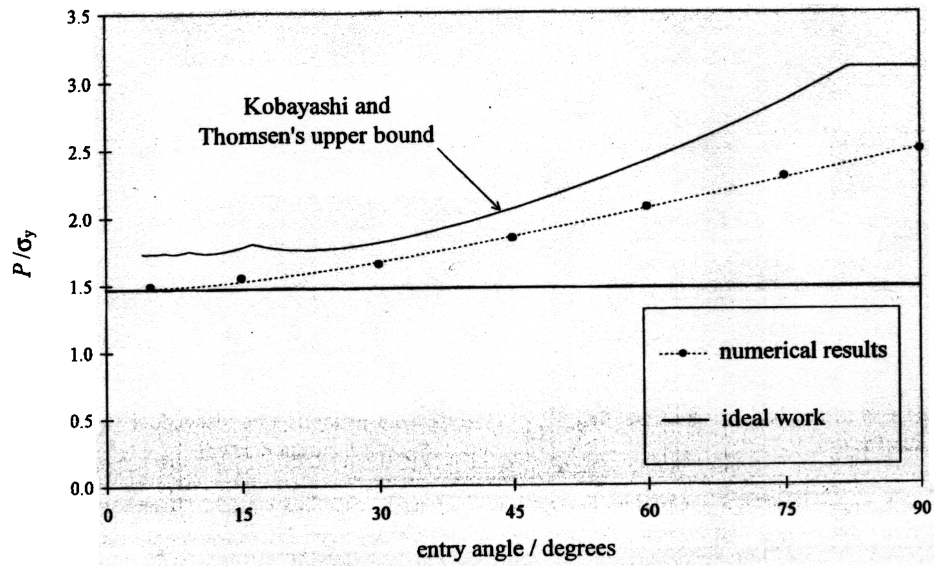

Fig. 8. Extrusion pressure against entry angle for axisymmetric extrusion through smooth, conical entry dies with a 52% diameter reduction.

believe there is a small error in Kobayashi and Thomsen's expression for the extrusion pressure, further details of which are given in an appendix. For angles greater than 82°, we have modified Kobayashi and Thomsen's solution, by introducing a static zone on the die face, in order to obtain a better (lower) upper bound. In this modified solution, the extrusion pressure is calculated for a conical entry die assuming a perfectly rough die face, and the entry angle is chosen so as to minimise the pressure. For the square entry die ($\psi = 90°$) this solution gives a rather higher extrusion pressure than that provided by Kudo's solution described above.

For large die angles, greater than about 45°, the calculated extrusion pressure varies approximately linearly with angle, but as the angle decreases the ideal work line is approached tangentially. A hyperbola may be fitted through the calculated points as follows:

$$P/\sigma_y = 1.47 + 0.496\{\sqrt{(1.85\psi)^2 + 1} - 1\} \quad (11)$$

where the die angle ψ is measured in radians. The initial constant in this equation is simply the ideal work contribution to the extrusion pressure from eq. (1).

DISCUSSION AND CONCLUSIONS

It is hoped that the work presented in this paper serves several purposes. Firstly, it provides an illustration of how the large deformation elastic–plastic finite-element method can be used to produce accurate solutions for flows of materials with a yield stress in extrusion geometries. The technique described, of which the remeshing process is an essential part, has great power due to its flexibility: different geometries, constitutive models and boundary conditions are all readily examined. Secondly, details of extrusion pressures are provided for a particular material model, namely the elastic, perfectly plastic solid, for a wide range of diameter reductions and entry angles in the axisymmetric configuration. These results have direct relevance to metal forming processes, to which the perfect plasticity model has been extensively applied, and potentially to the processing of soft solids, where it remains unclear whether there are any materials that are adequately described by such a model. Even in the absence of such materials, perfect plasticity can provide useful guidance for the construction of realistic models, as the yield behaviour is always an important feature of the flow of soft solids. Thirdly, the work may be thought to concern a purely hypothetical material, but with a detailed constitutive behaviour that is precisely known. The results can then be used to examine the Benbow–Bridgwater characterisation procedure, in order to determine the extent to which the characterisation parameters are independent of geometry, and to establish how they relate to the parameters of the constitutive model. It is this last theme that we wish to develop in these concluding remarks.

The characterisation parameter σ_0 is often taken to be a measure of the uniaxial yield stress σ_y, to which it is clearly closely related. However, the two quantities are not equal, and Fig. 7 provides a graphical representation of the relationship between them. The standard characterisation procedure described by Benbow and Bridgwater (1993) is equivalent to obtaining a point on the numerical results curve in Fig. 7, and drawing a straight line connecting this point to the origin; σ_0/σ_y is then half the slope of this line. Hence, σ_0 cannot be regarded as solely a material parameter, since it depends to some extent on geometry, particularly for diameter reductions of less than 50%. However, paste extrusion often involves very large reductions in the cross-sectional area of the flow, in which case ideal work forms the major contribution to the overall pressure drop, and it is perhaps for this reason that the Benbow–Bridgwater equation has been found to be a good basis for correlating the behaviour of pastes. In general, σ_0 will be an overestimate of the uniaxial yield stress of the material. For example, for a typical characterisation diameter ratio D_0/D of 25/3, σ_0 is 21% greater than σ_y.

Results for conical entry dies show that as the entry angle decreases from 90 to 0°, the deformation becomes closer to being homogeneous, and the extrusion pressure approaches the ideal work value. As the entry angle is altered, the extrusion pressure therefore only varies by the amount of redundant work associated with a square entry die. Again, for the large reductions encountered in paste extrusion most of the work done in a square entry die is ideal work, and the pressure is not expected to vary greatly with entry angle. This justifies the application of the Benbow–Bridgwater approach to conical as well as square entry dies, in cases where the reduction ratio is large. Conversely, for small reductions, most of the work done in a square entry die is redundant work, and σ_0 is expected to vary significantly with die angle.

Since a rate-independent model has been employed in the analyses, we have only been able to consider the σ_0 parameter in the die entry term of the Benbow–Bridgwater equation (the velocity factor α is identically zero). However, the results given in Figs 7 and 8 and by eqs (9)–(11) should also be appropriate for materials that display bulk rate dependence in the limit as the velocity of extrusion tends to zero, provided the condition of smooth walls still applies: if the largest rate of strain in the material is sufficiently small, the largest deviation from the initial yield stress is also small, and the stresses throughout the material are close to those for an ideal plastic having the same yield stress. In general, σ_0 may be expected to depend on wall friction in addition to die geometry, for both rate-dependent and rate-independent material models, although we have yet to investigate this effect.

Rate dependence is often an important feature of the behaviour of real pastes, and the velocity factor α is generally non-zero. Viscoplastic materials, displaying rate dependence in the bulk, could be modelled as Bingham or Herschel–Bulkley fluids, but with slip at the walls instead of the usual no-slip condition. They may therefore be described as lubricated Bingham or Herschel–Bulkley fluids. If the wall shear stress was assumed to be a function of the velocity of slip, rate dependence would also appear in the model via the boundary conditions. Analyses incorporating rate dependence of either kind would shed light on the velocity dependence in the die entry term of the Benbow–Bridgwater equation.

Acknowledgements

D. J. H. gratefully acknowledges the support of the U.K. Engineering and Physical Sciences Research Council and the Society of Chemical Industry.

NOTATION

a	length parameter in upper-bound velocity field
b	length parameter in upper-bound velocity field
D_0	barrel diameter
D	die land diameter
f	length ratio in upper bound velocity field
I	integral in upper-bound expression for extrusion pressure
L	die land length
n	number of pairs of velocity discontinuities in upper-bound velocity field
P_1	die entry pressure drop
P_2	die land pressure drop
P	overall pressure drop
r	radial coordinate
R_0	barrel radius
u	radial velocity component
v	axial velocity component
v_0	parameter in upper-bound velocity field
V	mean velocity of material in die land
W_0	initial width of sheet
W	final width of sheet
x	integration variable in upper-bound solution
y	integration variable in upper-bound solution
z	axial coordinate

Greek letters

α	Benbow–Bridgwater parameter characterising effect of velocity in die entry
β	Benbow–Bridgwater parameter characterising effect of velocity in die land
$\dot{\varepsilon}_{ij}$	strain rate tensor $[1/2(\partial u_i/\partial x_j + \partial u_j/\partial x_i)]$ where u_i is the velocity in direction x_i
$\dot{\bar{\varepsilon}}$	effective strain rate $[(2\dot{\varepsilon}_{ij}\dot{\varepsilon}_{ij})^{1/2}]$
μ	non-Newtonian fluid viscosity
ξ	reduction parameter $[\ln(D_0/D)]$
σ_l	longitudinal stress component
σ_y	uniaxial yield stress
σ_0	Benbow–Bridgwater parameter: initial bulk yield stress
τ_0	Benbow–Bridgwater parameter: initial wall stress in die land
τ_y	shear yield stress
ϕ	angle in upper-bound velocity field
ψ	entry angle

REFERENCES

Benbow, J. J. (1971) The dependence of output rate on die shape during catalyst extrusion. *Chem. Engng Sci.* **26**, 1467–1473.

Benbow, J. J. and Bridgwater, J. (1993) *Paste Flow and Extrusion*. Clarendon Press, Oxford, U.K.

Calladine, C. R. (1985a) *Plasticity for Engineers*, pp. 238–242. Ellis Horwood, Chichester, U.K.

Calladine, C. R. (1985b) *Plasticity for Engineers*, pp. 249–253. Ellis Horwood, Chichester, U.K.

Chakrabarty, J. (1987a) *Theory of Plasticity*, pp. 519–521. McGraw-Hill, Singapore.

Chakrabarty, J. (1987b) *Theory of Plasticity*, pp. 483–485. McGraw-Hill, Singapore.

Chakrabarty, J. (1987c) *Theory of Plasticity*, pp. 487–489. McGraw-Hill, Singapore.

Chen, C. C., Oh, S. I. and Kobayashi, S. (1979) Ductile fracture in axisymmetric extrusion and drawing. *Trans. ASME J. Engng Ind.* **101**, 23–44.

Feasey, J. F. and Wilson, A. J. (1996) *Chemical Engineering Tripos: Part 2.* Research Project Report, University of Cambridge, Cambridge.

Garvey, D. J. and Ross, R. J. (1996) *Chemical Engineering Tripos: Part 2.* Research Project Report, University of Cambridge, Cambridge.

Kobayashi, S. and Thomsen, E. G. (1965) Upper- and lower-bound solutions to axisymmetric compression and extrusion problems. *Int. J. Mech. Sci.* **7**, 127–143.

Kudo, H. (1960) Some analytical and experimental studies of axi-symmetric cold forging and extrusion—I. *Int. J. Mech. Sci.* **2**, 102–127.

Lee, E. H. (1977) Stress analysis of metal forming processes. In *Engineering Plasticity: Theory of Metal Forming Processes*, Vol. 1, ed. H. Lippmann, pp. 81–115. Springer, Vienna.

Lee, E. H. (1984) Finite deformation effects in plasticity analysis. In *Numerical Analysis of Forming Processes*, eds J. F. T. Pittman, O. C. Zienkiewicz, R. D. Wood and J. M. Alexander, pp. 373–386. Wiley, Chichester, U.K.

Lee, C. K. and Lo, S. H. (1994) A new scheme for the generation of a graded quadrilateral mesh. *Comput. Struct.* **52**, 847–857.

Lee, E. H., Mallett, R. L. and Yang, W. H. (1977) Stress and deformation analysis of the metal extrusion process. *Comp. Meth. Appl. Mech. Engng* **10**, 339–353.

Nagtegaal, J. C. and Veldpaus, F. E. (1984) On the implementation of finite strain plasticity equations in a numerical model. In *Numerical Analysis of Forming Processes*, eds J. F. T. Pittman, O. C. Zienkiewicz, R. D. Wood and J. M. Alexander, pp. 351–371. Wiley, Chichester, U.K.

Ovenston, A. and Benbow, J. J. (1968) Effects of die geometry on the extrusion of clay-like material. *Trans. Br. Ceram. Soc.* **67**, 543–567.

Peraire, J., Vahdati, M., Morgan, K. and Zienkiewicz, O. C. (1987) Adaptive remeshing for compressible flow computations. *J. Comput. Phys.* **72**, 449–466.

Voyiadjis, G. Z. and Foroozesh, M. (1991) A finite strain, total Lagrangian finite element solution for metal extrusion problems. *Comp. Meth. Appl. Mech. Engng* **86**, 337–370.

Zienkiewicz, O. C., Jain, P. C. and Oñate, E. (1978) Flow of solids during forming and extrusion: some aspects of numerical solutions. *Int. J. Solids Struct.* **14**, 15–38.

Zienkiewicz, O. C. and Zhu, J. Z. (1987) A simple error estimator and adaptive procedure for practical engineering analysis. *Int. J. Num. Meth. Engng* **24**, 337–357.

APPENDIX: AN UPPER-BOUND SOLUTION FOR AXISYMMETRIC EXTRUSION THROUGH CONICAL ENTRY DIES

Figure A1 shows a velocity field described by Kobayashi and Thomsen (1965) appropriate for axisymmetric extrusion through smooth-walled, conical entry dies. The velocity components in each region are given by

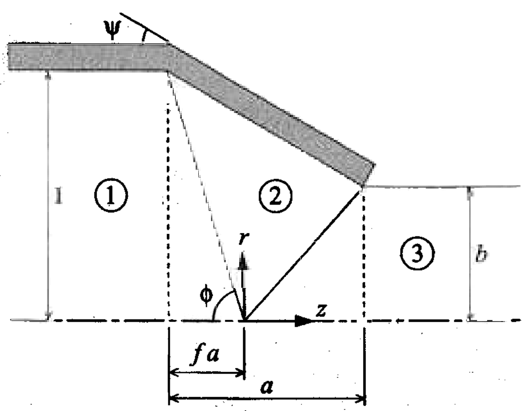

Fig. A1. Velocity field for axisymmetric extrusion through a conical entry die.

$$\text{Region 1} \quad u = 0, \quad v = 1$$

$$\text{Region 2} \quad u = -v_0\left(1 + \frac{z}{r}\tan\psi\right)\tan\psi,$$

$$v = v_0\left(1 + \frac{z}{r}\tan\psi\right) \tag{A1}$$

$$\text{Region 3} \quad u = 0, \quad v = \frac{1}{b^2}$$

where

$$v_0 = \frac{1}{(1 - fa\tan\psi)^2}.$$

For a material obeying von Mises' yield criterion, Kobayashi and Thomsen give the following expression for the extrusion pressure:

$$\frac{P}{\sigma_y} = \frac{\sin\psi}{\sqrt{3}}\left\{\frac{2}{\sin\phi\sin(\phi - \psi)} + \frac{\sqrt{2}}{\cos\psi}I\right\} \tag{A2}$$

where

$$I = \int_{-\cot\phi}^{\cot(\phi-\psi)} \frac{\sqrt{\{(\frac{1}{2} + 2\tan^2\psi)x^2 + x\tan\psi + (2 + \frac{1}{2}\tan^2\psi)\}}}{(1 + x\tan\psi)^2}\,dx \tag{A3}$$

and b and ϕ are assumed to be related by the constraint

$$b^{1/2} = \sin(\phi - \psi)/\sin\phi. \tag{A4}$$

By letting x equal z/r, similar expressions can be derived from the velocity field (A1) following the usual procedure for an upper-bound analysis (see e.g. Calladine, 1985). However, we believe there is a small error in Kobayashi and Thomsen's result, and that the integral (A3) should read

$$I = \int_{-\cot\phi}^{\cot(\phi-\psi)} \frac{\sqrt{\{(\frac{1}{2} + 2\tan^2\psi)x^2 + 3x\tan\psi + (2 + \frac{1}{2}\tan^2\psi)\}}}{(1 + x\tan\psi)^2}\,dx \tag{A5}$$

Making the substitution $y = (x - \tan\psi)/(x\tan\psi + 1)$, this can be written more compactly as

$$I = \int_{-\cot(\phi-\psi)}^{\cot\phi} \frac{\sqrt{2+\frac{1}{2}y^2}}{1 - y\tan\psi}\,\mathrm{d}y. \qquad \text{(A6)}$$

The integration can then be performed analytically, producing the rather cumbersome expression

$$\begin{aligned} I = {} & \cot\psi\left\{\sqrt{2+\tfrac{1}{2}\cot^2(\phi-\psi)} - \sqrt{2+\tfrac{1}{2}\cot^2\phi}\right\} \\ & - \frac{\cot^2\psi}{\sqrt{2}}\ln\left\{\frac{\sqrt{4+\cot^2(\phi-\psi)}+\cot(\phi-\psi)}{\sqrt{4+\cot^2\phi}-\cot\phi}\right\} \\ & + \cot\psi\sqrt{2+\tfrac{1}{2}\cot^2\psi} \qquad \text{(A7)} \\ & \times\ln\left\{\frac{\sin^2\phi}{\sin^2(\phi-\psi)} \frac{4\tan\psi+\cot\phi+\sqrt{(4+\cot^2\phi)(1+4\tan^2\psi)}}{4\tan\psi-\cot(\phi-\psi)+\sqrt{(4+\cot^2(\phi-\psi))(1+4\tan^2\psi)}}\right\}. \end{aligned}$$

In spite of the complexity of this result, the extrusion pressure is then readily evaluated with the assistance of a computer.

The constraint (A4), which defines the point on the axis where the velocity discontinuities meet, can be relaxed in order to obtain a better (lower) estimate for the extrusion pressure. ϕ is retained as an independent geometrical parameter, and the resulting expression for the extrusion pressure is minimised with respect to this variable. It does not appear that the optimum value of ϕ can be found analytically, but a numerical minimisation is accomplished relatively straightforwardly using a computer. This procedure has been used to obtain the upper-bound curve in Fig. 8.

The solution can be modified to allow for additional pairs of velocity discontinuities as shown in Fig. A2. For n pairs of discontinuities, b is replaced by $b^{1/n}$, and the extrusion pressure calculated from eq. (A2) is multiplied by n. The cusps on the upper-bound curve in Fig. 8 separate regions where the deformation modes have different values of the integer n.

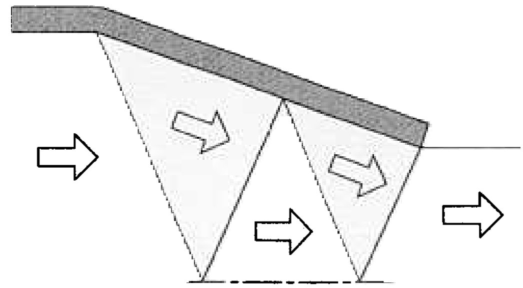

Fig. A2. Deformation mode for axisymmetric extrusion through a conical entry die with two pairs of velocity discontinuities ($n = 2$).